Comparative Biochemistry and Physiology, Part B 187 (2015) 71–77

Contents lists available at ScienceDirect

Comparative Biochemistry and Physiology, Part B

journal homepage: www.elsevier.com/locate/cbpb

Characterization of carbonic anhydrase XIII in the erythrocytes of the Burmese python, *Python molurus bivittatus*

A.J. Esbaugh [a,*], S.M. Secor [b], M. Grosell [c]

[a] Department of Marine Science, University of Texas at Austin, Marine Science Institute, 750 Channel View Drive, Port Aransas, TX 78418, USA
[b] Department of Biological Sciences, University of Alabama, Tuscaloosa, AL 35487-0344, USA
[c] Division of Marine Biology and Fisheries, University of Miami, Rosenstiel School of Marine and Atmospheric Science, 4600 Rickenbacker Causeway, Miami, FL 33149, USA

ARTICLE INFO

Article history:
Received 16 March 2015
Received in revised form 8 May 2015
Accepted 11 May 2015
Available online 22 May 2015

Keywords:
Red blood cells
CA XIII
CA I
Carbonic anhydrase isoforms
Specific dynamic action

ABSTRACT

Carbonic anhydrase (CA) is one of the most abundant proteins found in vertebrate erythrocytes with the majority of species expressing a low activity CA I and high activity CA II. However, several phylogenetic gaps remain in our understanding of the expansion of cytoplasmic CA in vertebrate erythrocytes. In particular, very little is known about isoforms from reptiles. The current study sought to characterize the erythrocyte isoforms from two squamate species, *Python molurus* and *Nerodia rhombifer*, which was combined with information from recent genome projects to address this important phylogenetic gap. Obtained sequences grouped closely with CA XIII in phylogenetic analyses. *CA II* mRNA transcripts were also found in erythrocytes, but found at less than half the levels of *CA XIII*. Structural analysis suggested similar biochemical activity as the respective mammalian isoforms, with CA XIII being a low activity isoform. Biochemical characterization verified that the majority of CA activity in the erythrocytes was due to a high activity CA II-like isoform; however, titration with copper supported the presence of two CA pools. The CA II-like pool accounted for 90 % of the total activity. To assess potential disparate roles of these isoforms a feeding stress was used to up-regulate CO_2 excretion pathways. Significant up-regulation of *CA II* and the anion exchanger was observed; *CA XIII* was strongly down-regulated. While these results do not provide insight into the role of CA XIII in the erythrocytes, they do suggest that the presence of two isoforms is not simply a case of physiological redundancy.

1. Introduction

Carbonic anhydrase (CA) is a ubiquitously expressed metalloenzyme that catalyses the hydration and dehydration reactions of carbon dioxide and bicarbonate, respectively. This basic reaction has innumerable physiological and biochemical associations and consequently CA isoforms are found in virtually all living organisms. These isoforms are divided into three different gene families – α, β, and γ – however all vertebrate CA isoforms belong to the α-CA gene family (Hewett-Emmett, 2000; Hewett-Emmett and Tashian, 1996). At present, this gene family consists of 16 different mammalian isoforms (Frost, 2014) with additional non-mammalian members (Esbaugh et al., 2004, 2005, 2009; Esbaugh and Tufts, 2006a), all of which have distinct kinetic properties and sub-cellular locations (Chegwidden and Carter, 2000; Frost, 2014; Henry, 1996). The members of the α-CA gene family can generally be divided into three distinct groups based on a combination of molecular properties and sub-cellular location (Esbaugh and Tufts, 2006b; Frost, 2014). One group includes the membrane-bound isoforms (IV, IX, XII, XIV and XV), while a second contains non-catalytic CA-related proteins (VIII, X, and XII). The final and most recognized group includes those isoforms found in the cytoplasm (I, II, III, VII and XIII) or mitochondria (Va and Vb).

The best known role for cytoplasmic CA is in the erythrocytes where it was first discovered (Brinkman et al., 1932; Meldrum and Roughton, 1933). Cellular aerobic metabolism produces carbon dioxide that diffuses into capillaries and subsequently into erythrocytes following a partial pressure gradient. CA, one of the most abundant proteins in the erythrocytes, acts to facilitate carbon dioxide hydration to maintain and maximize the CO_2 diffusion gradient into the erythrocytes by quickly hydrating carbon dioxide to form bicarbonate and protons. The resulting bicarbonate ions are shuttled out the cell by the anion exchange protein band 3 (AE1, *slc4a1*), while the resulting proton is buffered by its attachment to hemoglobin contributing to the Bohr Effect (reviewed by Perry et al., 2009; Swenson, 2000; Tufts and Perry, 1998). This combination of events helps to maintain the partial pressure gradient necessary for the diffusion of carbon dioxide from tissues to blood. At the respiratory epithelium these processes are reversed; CA catalyses the formation of carbon dioxide, which diffuses out of the erythrocytes and across the respiratory membrane. This pathway is common to all vertebrates with the exception of agnathans whose

* Corresponding author. Tel.: +1 361 417 6835.
E-mail address: a.esbaugh@austin.utexas.edu (A.J. Esbaugh).

http://dx.doi.org/10.1016/j.cbpb.2015.05.006
1096-4959/

erythrocytes lack the rate-limiting anion exchange capabilities (Ellory et al., 1987; Tufts et al., 1992).

The majority of vertebrate erythrocytes contain two distinct CA isoforms (Esbaugh and Tufts, 2006b; Frost, 2014), although the agnathans appear to have only a single isoform (Esbaugh and Tufts, 2006a). Mammalian erythrocytes contain both a high activity CA II and low activity CA I isoform, while teleost species contain two high activity isoforms (Esbaugh et al., 2005). However, teleosts are unique from mammals in that one isoform is tissue specific (CA-b). The available evidence therefore suggests that high activity cytoplasmic isoforms appeared early in vertebrate evolution, and the plethora of current isoforms arose as a consequence of subsequent gene/genome duplication events (Esbaugh and Tufts, 2006a,b; Hewett-Emmett, 2000; Hewett-Emmett and Tashian, 1996). Interestingly, fish and tetrapod vertebrate isoforms are phylogenetically distinct, which suggests that the duplication events occurred after the divergence of these groups (Esbaugh et al., 2004, 2005; Gilmour et al., 2009; Lund et al., 2002); however, there remain a number of important gaps in our understanding of the evolution of erythrocyte CA and proliferation of cytoplasmic CA isoforms. One such gap is an almost complete absence of information regarding cytoplasmic CA in reptiles. What little is known relates mostly to the identification of pulmonary CA IV-like isoforms (Stabenau et al., 1996; Stabenau and Heming, 2003; Stabenau and Vietti, 2002) with the exception of a partial biochemical characterization of erythrocyte CA from terrapin turtles (*Malaclemys terrapin*) (Hall and Schraer, 1979).

On this background, the current study was undertaken to provide insight into the distribution and function of cytoplasmic CA isoforms in the erythrocytes of Burmese pythons, *Python molurus bivittatus*. The first objective was to characterize the erythrocyte CA pool using a combination of molecular sequencing and biochemical assays. The obtained molecular information was then combined with data from recent reptile genome projects – as well as novel sequence information from the erythrocytes of a second snake species, *Nerodia rhombifer* – to perform a complete phylogenetic and structural assessment of cytoplasmic CA isoforms in reptiles as compared with other vertebrates. Finally, transcriptional regulation of erythrocyte CA in Burmese pythons after a large meal feeding event was used to assess the role of the various erythrocyte CA isoforms in CO_2 transport.

2. Materials and methods

2.1. Experimental animals and sampling

Captive-born hatchling Burmese pythons (*P. molurus bivittatus*) were purchased commercially and housed individually in 20-l plastic containers at 27 °C under a 14 h:10 h light:dark cycle. Snakes (both male and female) were fed laboratory rats every 2 weeks and had continuous access to water. Prior to the study 12 pythons (mean ± S.E.M. = 501 ± 10 g) were fasted for approximately 30 days to insure that they were post-absorptive (Secor and Diamond, 1995). Six snakes remained fasted for the study and 6 pythons were fed a single prekilled rat weighing approximately 25% of the snake's body mass. Snakes were euthanized fasted or at 3 days post-feeding (dpf) by severing their spinal cord immediately posterior to the head. From a mid-ventral incision blood was sampled directly from the severed left systemic artery. Blood samples were immediately centrifuged and the plasma frozen in liquid nitrogen while erythrocytes were washed with saline then frozen. All samples were subsequently stored at −80 °C.

2.2. Molecular methods

Total RNA was extracted from python erythrocytes using RNA Stat-60 reagent according to manufacturer guidelines (Tel-test Inc, TX, USA). Total RNA was quantified using an ND-1000 (Thermo Fisher Scientific, DE, USA) spectrophotometer at a wavelength of 260 nm. Prior to cDNA synthesis, RNA was DNase-treated with amplification grade DNase I (Invitrogen, CA, USA) to remove DNA contamination. Subsequent cDNA synthesis was performed using RevertAid reverse transcriptase according to manufacturer specifications (Fermentas, MD, USA). Degenerate primers were designed for cytoplasmic CA by aligning available sequences from a diverse array of vertebrates and identifying conserved nucleotide regions (Table 1). PCR reactions were performed according to standard protocols using commercial Taq DNA polymerase and buffer (Qiagen, CA, USA). PCR products were subsequently gel extracted using the Qiaquick kit (Qiagen, CA, USA), cloned (TOPO TA cloning kit; Invitrogen, CA. USA) and sequenced. Primers for rapid amplification of cDNA ends (RACE) and real-time PCR were designed using the fastpcr freeware program (Table 1). RACE libraries were generated using the SmartRace cDNA synthesis kit (Clontech, CA, USA). Real-time PCR was performed on an Mx3000P real-time PCR system (Stratagene, CA, USA) using the Brilliant SYBR green master mix kit (Stratagene, CA, USA; 12.5 μl reactions). Both the thermocycler setup and reaction composition were performed according to manufacturer guidelines, and a disassociation curve was used to assess the primer specificity of each reaction. The PCR efficiency of each primer pair was calculated using a cDNA standard curve. PCR efficiencies ranged from 96 to 114% with an $R^2 \geq 0.98$. Relative mRNA transcript abundance was calculated using the delta-delta ct method using elongation factor 1α (ef1α) as an internal control and the fasted treatment as the relative control (Pfaffl, 2001). Successful DNase treatment was verified using a no reverse transcriptase control.

2.3. Biochemical methods

CA activity was measured using the electrometric delta pH method (Henry, 1991). Briefly, the reaction medium consisted of 2.5 ml of buffer (225 mM mannitol, 75 mM sucrose, 10 mM Tris base; Sigma, MO, USA) kept at 4 °C. Biochemical assessments of python and bovine erythrocyte CA were performed using 2 ml of buffer. The reaction was started by adding 100 μl of CO_2 saturated Milli-Q water using a gas tight Hamilton syringe. The reaction rate was measured over a pH change of 0.15 units (+10 mV). To calculate the true catalyzed reaction rate, the uncatalyzed reaction rate was subtracted, and the buffer capacity was used to convert the rate from mV into mol H^+ per unit time. The pH was measured using a PHC4000 combined pH electrode (Radiometer Analytical, Lyon, France) attached to a PHM220 lab pH meter (Radiometer Analytical, Lyon, France) connected to a computer for data collection.

CA assay measurements were performed on erythrocytes from fasted and 3 dpf snakes, while biochemical characterization was performed only on fasted snakes. Red blood cell lysates were prepared by the addition of 500 volumes of Milli-Q water and bovine red blood cell lysates were prepared from commercially available lyophilized protein (Sigma-Aldrich, MO, USA). For determination of inhibitor characteristics the activity of a set volume of lysate was assayed in the presence of varying concentrations of inhibitor, including acetazolamide, copper ($CuSO_4$) and CNO^- (KCNO) (all chemicals from Sigma-Aldrich).

Table 1
List of primers used for real-time and degenerate PCR. All sequences are 5′ to 3′ and reverse primers are reverse compliments of the genetic sequence.

Application	Gene	Orientation	Sequence
Degenerate	*CA*	Forward	CAG TTC CAY TTC CAY TGG G
		Reverse	RAC GAT CCA KGT GAC RCT CTC
Real-time	*CA XIII*	Forward	GTT GAA GCT GCT CGG CAA TCT G
		Reverse	GGG ACT GTG AGA GAC CCA AGG
	CA II	Forward	ATG TCC TGG GGC TAC AGC AA
		Reverse	GTG CAG GAT CGA ACT TGG CA
	AE1	Forward	TCT CTG GTG CTC ATG GGA GG
		Reverse	CAA TCA CCC GTC GAA GCT TGC
	Ef1α	Forward	TCT CGA TTC TGT GGG TGG T
		Reverse	CTC AAT CTC GTG TGG CTG A

Inhibitor constants were calculated using a Dixon plot (Dixon, 1953) for copper and CNO^-, while an Easson–Stedman plot (Easson and Stedman, 1937) was used for acetazolamide. The catalytic rate constant of red blood cell lysates was determined using the method of Maren et al. (1960). Briefly, lysates were assayed in the presence of varying concentrations of substrate allowing for the construction of a Lineweaver–Burke plot to calculate maximal velocity. The enzyme concentration was then determined from the y-intercept of the acetazolamide inhibition plots. For both python and bovine lysates, a ratio of enzyme units to enzyme concentration was calculated from acetazolamide plots so concentration could be easily obtained via enzyme unit calculations. The catalytic rate constant (k_{cat}) was then determined by dividing maximal velocity by concentration. For copper analyses enzyme units in the assay chamber ranged from 3.69 to 5.88, while enzyme units were kept between 1 and 2 for all other analyses. All enzyme assay results were normalized to total protein content, which was detected using a commercially available Bradford assay reagent (Sigma Aldrich).

2.4. Phylogenetic analysis

A total of 48 CA sequences were mined from Genbank, which included isoforms from all five vertebrate classes. All phylogenetic analyses were performed using MEGA version 6.06 and amino acid alignments were performed using the MEGA Clustal alignment tool. Three distinct analyses were performed: 1) neighbor joining (NJ), 2) maximum parsimony (MP) and 3) maximum likelihood (ML). Gaps were treated as complete deletion for parsimony and likelihood methods and pairwise deletion for neighbor joining methods. MP was performed using the subtree-pruning-regrafting (SPR) method, while ML was performed using a Jones–Taylor–Thornton (JTT) substitution model. Both methods used the MEGA default tree inference options. NJ was performed using the Poisson substitution model. Support for nodes in all analytical procedures was performed via bootstrap analysis with 1000 replications. For all resulting trees, the *Drosophila melanogaster* CA sequence was used to root the analysis.

2.5. Statistics

Comparisons of mRNA abundance and biochemical parameters between fasted and 3 dpf pythons were performed using an unpaired Student's *t*-test except in cases where normality was not met and a non-parametric Mann–Whitney rank sum test was performed. Gene transcript data were log transformed prior to statistical analysis. A fiducial level of significance of 0.05 was used for all statistical analyses.

3. Results

3.1. Sequence analysis

Homology cloning techniques were performed to isolate erythrocyte CA transcripts from the Burmese python and the diamond back watersnake. Transcripts with coding regions of 777bp and 801 bp were obtained, respectively. When these genes were included in a phylogenetic analysis of cytoplasmic CA isoforms both grouped within the

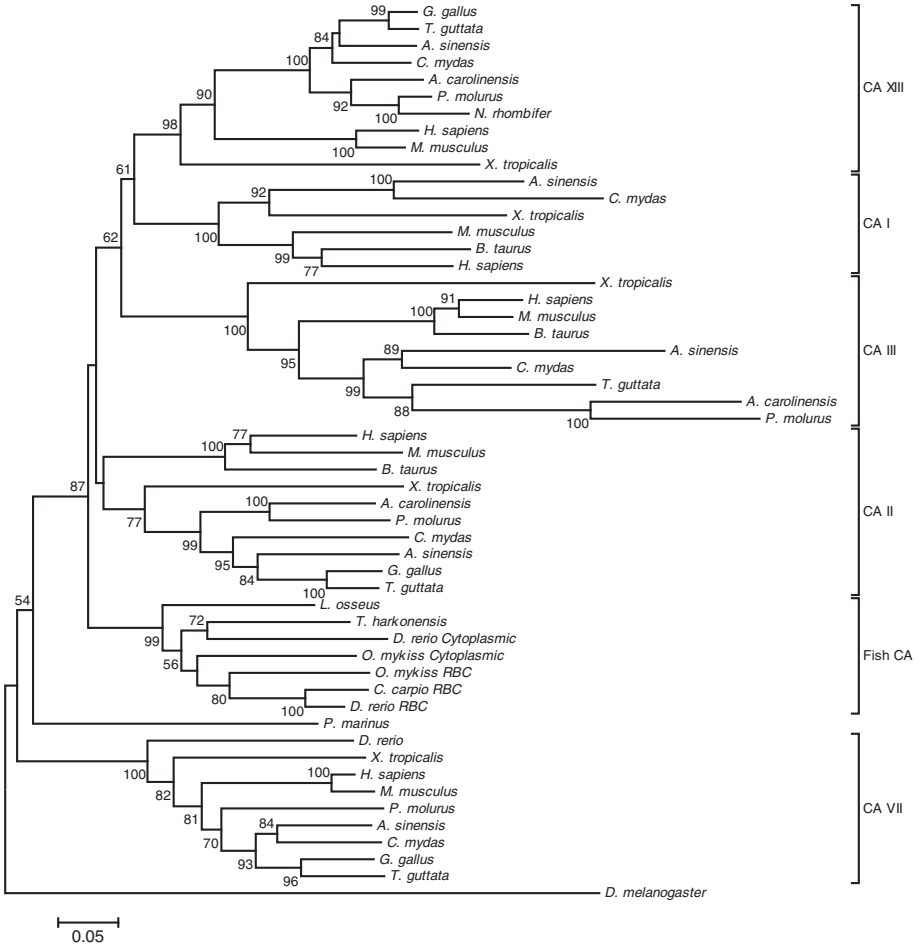

Fig. 1. A neighbor-joining phylogenetic reconstruction of the cytoplasmic α-carbonic anhydrase isoforms. Bootstrap values for nodes are denoted with the exception of values below 50%, which indicates poor node support. Branch lengths are drawn to scale with 0.05 equating to 5% amino acid replacement in the protein alignment. Similar topology was obtained with maximum likelihood and maximum parsimony reconstruction methods.

vertebrate CA XIII group (Fig. 1), most closely with isoforms from other squamate reptile species. This evolutionary pattern was consistent for other CA isoforms, with *Anolis carolinensis* (American green anole) consistently grouping with the python, while the *Alligator sinensis* (Chinese alligator) and *Chelonia mydas* (Green sea turtle) grouped with avian species. Interestingly, the erythrocyte CA I isoform was not found for squamate species, but was found for both *A. sinensis* and *C. mydas*. Note that all three phylogenetic methods (MP, ML and NJ) provided trees of similar topology (data not shown). The only notable difference between trees was the placement of the *X. tropicalis* CA II sequence, which was grouped with other non-mammalian CA II sequences in NJ analysis and MP analysis. Conversely, ML analysis placed it basal to all non-CA VII isoforms. However, the ML tree had poor bootstrap support (<50) with respect to the relevant nodes.

A detailed examination of the active site pocket for select reptile cytoplasmic CA isoforms was performed to assess theoretical activity (Table 2). The five CA XIII isoforms all contained the characteristic Thr/Val-199 substitution. The active site of the CA II isoforms was generally conserved when compared to the mammalian consensus sequence, with all modification occurring at non-crucial residues. The active site pocket of the *A. sinensis* and *C. mydas* CA I isoforms contained the characteristic Asn/His-67 and Thr/His-200 substitutions. In general, the structural properties of the various reptile isoforms were consistent with their mammalian counterparts, suggesting conserved biochemical properties.

3.2. Biochemical analysis

Erythrocyte lysates from *P. molurus* were used to compare the dominant biochemical properties to commercially obtained bovine CA II (Table 3). The turnover number and substrate affinity constant for the two CA pools were comparable. Similarly, the sensitivity to the inhibitor acetazolamide was alike in both pools, although the python pool was slightly more sensitive. The CNO^- anion inhibitor – known to be 100× more potent against CA II than CA XIII – was only slightly more effective against the python CA pool. Titration of python erythrocyte CA activity with copper resulted in a bi-modal response (Fig. 2). The dominant CA pool accounted for about 85–90% of the activity and had a K_i similar to mammalian CA II. Interestingly, the less abundant CA pool had a K_i similar to the low activity CA I found in mammalian erythrocytes.

3.3. Transcriptional analysis

The relative transcript abundance of *CA XIII*, *CA II* and the anion exchanger *slc4a1* (*AE1*) was assessed using real-time PCR, with *CA XIII* found to be 2.5 times more abundant than *CA II* and 10 times more abundant than *AE1* (Fig. 3). Interestingly, a differential response between *CA II*/*AE1* and *CA XIII* was observed after animals were fed a meal comprising 25% of their body weight – a known respiratory and acid–base stressor related to specific dynamic action and alkaline tide. At 3 days post-feeding the transcripts for both *CA II* and *AE1* were significantly up-regulated by 0.6 and 0.7-fold, respectively, while *CA XIII* was down-regulated by 2.5-fold. Feeding also resulted in a down-regulation of the red blood cell CA activity pool by approximately 10% (Fig. 4).

4. Discussion

The vast majority of vertebrates possess high activity cytoplasmic CA activity, which is integral for maintaining carbon dioxide excretion at the respiratory epithelium and enhancing transport in the tissues. Interestingly, the identity of erythrocyte CA isoforms is not consistent across vertebrate groups. Most mammals contain both a low activity CA I isoform and a high activity CA II isoform, the latter of which is responsible for the majority of the observed activity (Maren et al., 1976). Conversely, fish erythrocytes contain two phylogenetically distinct isoforms, a erythrocyte specific isoform (CA-b) and a general cytoplasmic isoform (CA-c) with approximately 300-fold lower mRNA abundance (Esbaugh et al., 2005). Although the available information for non-mammalian tetrapods is more sparse, it appears that amphibians and birds have only a high activity isoform (Sanyal, 1984), while turtles

Table 2
Analysis of the putative active site pocket sequences for reptile cytoplasmic carbonic anhydrase isoforms as compared to the high activity human carbonic anhydrase II. Numbers represent the location of each respective amino acid relative to alignment with human carbonic anhydrase II. Amino acid substitutions are designated by the respective amino acid letter, while no change is denoted by a dot.

Consensus II		Y	S	N	N	H	S	F	N	E	I	Q	H	H	E	H	E	H	V	F	L	V	G	W	Y	L	T	T	P	P	L	C	V	W	V	N	R
		7	29	61	62	64	65	66	67	69	91	92	94	96	106	107	117	119	121	131	141	143	145	192	194	198	199	200	201	202	204	206	207	209	211	244	246
						+							z	z				z	~		~	~				~	*							~	~			
A. sinensis	I	.	.	.	.	.	.	.	H	N	R	.	.	.	.	.	.	.	.	I	.	I	T	.	.	.	.	H	.	.	Y	S	.	.	I	.	.
	II	.	.	.	.	.	.	.	.	.	.	.	.	.	.	.	.	.	.	.	.	.	.	.	.	.	.	.	.	.	.	.	.	.	.	.	.	.
	III	A	T	.	.	R	T	C	R	V	R	.	.	.	.	.	.	.	.	.	V	I	.	.	.	F	.	.	.	.	E	.	.	.	L	.	.
	XIII	.	.	.	.	.	.	T	S	.	R	.	.	.	.	.	.	.	.	.	.	.	A	.	.	.	.	V	.	.	.	S	.	.	.	.	.
C.mydas	I	.	.	.	V	.	.	.	H	N	H	.	.	.	.	.	.	.	.	.	.	.	A	.	.	.	.	H	.	.	F	S	I	.	I	.	.
	II	.	.	.	.	.	.	.	.	.	.	.	.	.	.	.	.	.	.	.	.	.	.	.	.	.	.	.	.	.	F	.	.	.	.	.	.
	III	.	.	.	.	R	T	C	R	V	R	.	.	.	.	.	.	.	.	.	V	.	.	.	.	F	.	.	.	.	E	.	.	.	L	.	.
	XIII	.	.	.	.	.	.	T	S	.	R	.	.	.	.	.	.	.	.	.	.	.	A	.	.	.	.	V	.	.	L	S	I	.	I	.	.
A. carolinensis	II	.	.	.	.	.	.	.	.	.	K	.	.	.	.	.	.	.	.	.	.	.	.	.	.	.	.	.	.	.	.	.	.	.	.	.	.
	III	.	.	.	T	K	G	C	R	A	R	.	L	.	.	.	.	Q	.	Y	A	I	A	Y	.	F	.	.	.	.	E	.	.	.	I	.	.
	XIII	.	.	.	.	.	.	T	S	.	R	.	.	.	.	.	.	.	.	.	.	.	A	.	.	.	.	.	.	.	.	S	.	.	I	.	.
P. molurus	II	.	.	.	.	.	.	.	.	V	K	.	.	.	.	.	.	.	.	I	.	.	.	.	.	.	.	.	.	.	.	.	.	.	.	.	.
	III	.	.	.	T	K	T	L	R	A	R	.	.	.	.	.	.	.	.	Y	V	T	A	Y	.	F	.	.	.	.	E	.	.	.	L	.	.
	XIII	.	.	.	.	.	.	T	S	.	R	.	.	.	.	.	.	.	.	.	.	.	A	.	.	.	.	V	.	.	.	S	.	.	.	.	.
N. rhombifer	XIII	.	.	.	.	.	.	T	S	.	R	.	.	.	.	.	.	.	.	L	.	.	A	.	.	.	.	V	.	.	.	S	.	.	I	.	.

z = zinc binding ligand
+ = proton shuttling ligand
~ = substrate associated pocket
* = Thr-199 loop site

Table 3
Kinetic parameters of red blood cell carbonic anhydrase isoforms from *P. molurus* compared to known mammal isoforms. All *P. molurus* measurements are mean ± SEM ($N = 3$), while bovine measurements are from a single commercially obtained source.

Enzyme source		K_i Az (nM)	K_i Cu (μM)	K_i CNO (μM)	Kcat (e^4 s^{-1})	Km (mM)
Python	High	0.64 ± 0.2	0.4 ± 0.1	2.4 ± 0.6	1.3 ± 0.6	21.5 ± 8.5
	Low		30.9 ± 14.5			
Bovine	CA II	1.87	1.2 [a]	6.5	4.1	17.1
	CA I		36.2 [a]			

[a] From Lund et al., 2002. Assayed using the delta pH method at 4 °C.

appear to be similar to mammals (Hall and Schraer, 1979). The results from the current study suggest that two squamata species, *P. molurus* and *N. rhombifer*, contain an erythrocyte isoform distribution that is unique from other vertebrates. Specifically, these two snake species contain at least two CA isoforms with one being CA XIII, which has not previously been linked to erythrocytes.

The CA isoforms obtained by homology cloning were combined with cytoplasmic CA isoforms from recent reptile genome projects (*A. sinensis, C. mydas, P. molurus* and *A. carolinensis*) to more fully assess evolutionary aspects of cytoplasmic CAs in reptiles. It is generally accepted that gene duplication of a high activity ancestral CA isoform gave rise to CA I, II, III and XIII (Lehtonen et al., 2004), which took place after the divergence of fish and tetrapod vertebrates (Esbaugh and Tufts, 2006a,b). The presence of CA I, II, III and XIII in reptiles and amphibians is consistent with this hypothesis and suggests that these gene duplication events took place prior to the divergence of the different tetrapod groups. The presence of all four isoforms in amphibians is particularly convincing as these are thought to be the most basal tetrapod class. The conserved active site structure of the reptile CA isoforms also suggests that they are biochemically similar to their mammalian counterparts. Specifically, CA II is remarkably conserved when compared to the consensus mammalian CA II active site structure, supporting the designation as a high activity isoform. Conversely, reptile CA III shows poor conservation of the active site structure, including amino acid substitutions at important residues including the proton shuttle His-64 residue and several components of the substrate associated pocket. This is similar to mammalian CA III, which is a very low activity isoform whose physiological function is thought to be largely independent of catalytic activity (reviewed by Frost, 2014).

The available evidence suggests that CA I is not present in squamate reptiles, but is present in testudinian and crocodilian reptiles. No evidence for this isoform could be found in the *P. molurus* or *A. carolinensis* genomes and homology cloning efforts to amplify this sequence from *P. molurus* and *N. rhombifer* proved fruitless. Importantly, CA I is typically found in much higher abundance in erythrocytes than CA II, so it seems likely that such an isoform would have been identified through our efforts, or genome projects, had it been present. The current analysis suggests that CA I may also be absent from bird species as no evidence could be found in either the *Gallus gallus* or *Taeniopygia guttata* genome. It is tempting to suggest that CA I may have been lost at a single point during reptilian evolution and this trait was subsequently carried into the avian lineage; however, squamate reptiles are a sister taxa to the archosaur group that includes birds and crocodiles. Given that CA I is found in crocodiles, as well as the more basal turtles, it seems likely that the loss of CA I in squamates and birds is the result of independent evolutionary events.

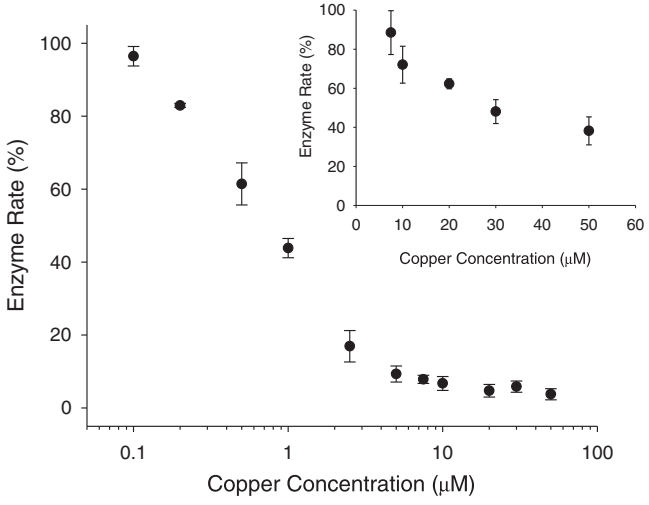

Fig. 2. A) A representative plot of the effects of copper inhibition on red blood cell carbonic anhydrase activity from *P. molurus*. Inset: Inhibition plot highlighting the less copper sensitive pool of red blood cell carbonic anhydrase.

The low activity of CA I is caused by the substitution of histidine at residues 67 and 200, which alters the shape of the active site pocket and subsequently shifts the rate limiting proton shuttle mechanism (Boone et al., 2014; Lindskog and Silverman, 2000). These substitutions are found in the alligator and turtle CA I. Interestingly, mammalian CA XIII is known to have similar catalytic activity as CA I, despite a relatively conserved active site pocket (Innocenti et al., 2004; Lehtonen et al., 2004). It is believed that low activity in CA XIII is the result the Thr/Val-200 substitution, which is found within the important Thr-199 loop motif that is critical for orienting the zinc-bound hydroxide within the active site. By changing the orientation of the zinc-bound hydroxide, the valine substitution is hypothesized to alter the efficiency of the proton shuttle mechanism. The Thr/Val-200 substitution previously described for murine CA XIII is also found in the sequences of all reptiles examined; in fact, this substitution is found in all the available CA XIII sequences and appears to be a hallmark characteristic of this isoform.

It is tempting to suggest that CA XIII replaced CA I in the erythrocytes of squamate reptiles, and this hypothesis is reinforced by the biochemical and transcriptional data. Like CA I in mammals, CA XIII is found in higher amounts than CA II, assuming mRNA transcript abundance is representative of protein abundance. Also like mammals, the biochemical properties of erythrocyte lysates are dominated by CA II activity. As shown in Table 2, the catalytic rate and substrate affinity constant of python erythrocyte lysates resemble those of bovine CA II. Similarly the CNO^- and acetazolamide inhibitor characteristics resemble CA II. Perhaps the most telling data are those for copper inhibition, which provide evidence for two independent pools of erythrocyte CA. The majority of CA activity has a copper inhibition constant similar to mammalian CA II; however, a second pool that accounts for approximately 10% of the total activity responded more similar to the low activity CA I isoform. Importantly, copper is known to inhibit activity through action on the proton shuttle mechanism (Eriksson et al., 1988; Magid, 1967), so it seems likely that copper would inhibit CA XIII similar to CA I as changes to the proton shuttle mechanism are also responsible for the lower overall activity of both isoforms. From an evolutionary perspective, it is interesting to speculate on the sequence of events that would result in CA XIII functionally replacing CA I in the erythrocytes of squamate reptiles. One possibility is the introduction of an erythrocyte targeting promoter sequence into the promoter region of CA XIII, such as the GATA1 consensus sequence (Ferreira et al., 2005). Interestingly, the consensus GATA1 sequence is found approximately 1000 bp upstream of the python CA XIII transcription start site. This could establish the physiological redundancy that would allow for the CA I gene to be lost.

The physiological requirement for two cytoplasmic CA isoforms in the erythrocytes of vertebrates is unclear. There are no apparent detrimental effects on carbon dioxide transport in those few species with only one of the two isoforms (Yang et al., 2000), which is similar for human CA I deficiency syndrome (Frost, 2014). One possibility is that the two isoforms simply act as a physiological redundancy for a particularly important function; however, the conserved pattern of erythrocyte CA isoform distributions across all vertebrate groups makes this

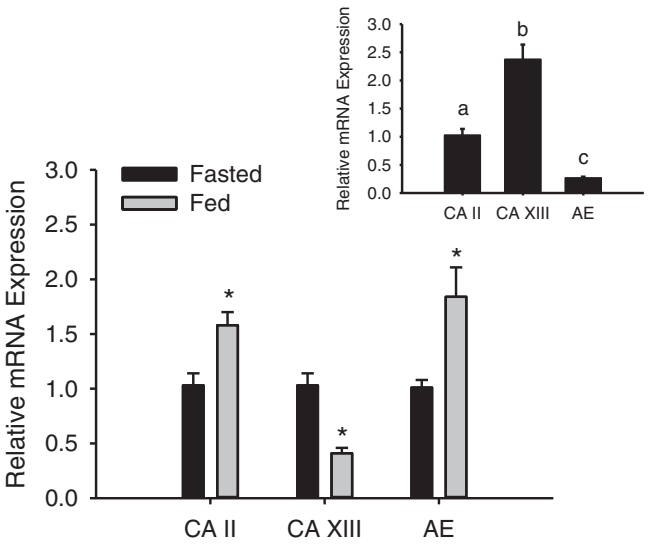

Fig. 3. The effect of feeding on mRNA abundance in the red blood cell of *P. molurus* as detected by real-time RT-PCR. A significant difference between fasted and fed treatments is denoted by an asterisk (unpaired Student's *t*-test, or Mann–Whitney rank sign test, $P < 0.05$). Inset: Relative abundance of red blood cell gene transcripts in fasted *P. molurus* as normalized to carbonic anhydrase II. Significantly different transcript abundances. All values are mean ± S.E.M. ($N = 5–6$).

explanation unsatisfying. Furthermore, both fish and squamate reptiles use different CA isoforms from those found in other vertebrates, which suggests that the physiological function was adopted multiple times. To gain some insight into this phenomenon, we employed a common physiological stress that enhances gas transport in an effort to stimulate transcriptional regulation of erythrocyte carbon dioxide pathways. As a sit-and-wait predator, pythons eat large meals at infrequent intervals (Greene, 1997; Pope, 1961; Secor and Nagy, 1994; Slip and Shine, 1988). Consequently, pythons have a suite of physiological adaptations that regulate digestive performance, one of which is a substantial postprandial specific dynamic action that greatly enhances metabolic rate and results in a 10-fold increase in carbon dioxide excretion rates (Hicks and Bennett, 2004; Secor et al., 2000). Importantly, respiratory stress has been shown to result in transcriptional regulation of erythrocyte machinery in other non-mammalian vertebrates (Esbaugh et al., 2005). Interestingly, a 25% body weight meal resulted in the expected, albeit small, up-regulation of both CA II and the band 3 anion exchange protein, but resulted in a more substantial down-regulation in CA XIII. The overall effect on erythrocyte CA activity was an approximately

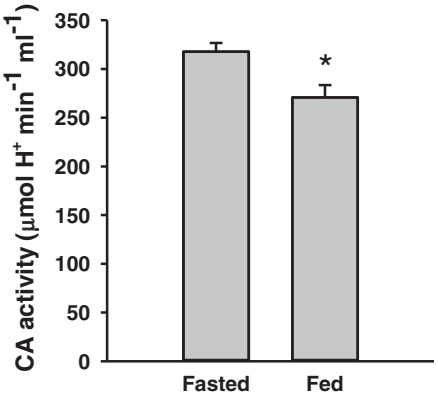

Fig. 4. Cytoplasmic carbonic anhydrase activity in fasted and postprandial *P. molurus* red blood cell lysates. A significant difference between fasted and fed treatments is denoted by an asterisk (unpaired Student's *t*-test, or Mann–Whitney rank sign test, $P < 0.05$). All values are mean ± S.E.M. ($N = 6$).

10% decrease, which coincides with the previous suggestion that CA XIII makes up a relatively small pool of the total activity. It is also important to note that while the targeted destruction of CA XIII could likely occur quickly, up-regulation of CA II would suffer from lags stemming from zinc limitations at the post-transcriptional level (Mitchell and Henry, 2014). This may explain why the overall activity is down-regulated despite an up-regulation of CA II.

While the differential transcriptional responses do not highlight a specific role for CA XIII in the erythrocytes of pythons, the available evidence would suggest that its primary function is not carbon dioxide excretion. It is possible that the role of CA XIII is related to the sub-cellular localization and functional association with other proteins in the erythrocyte. However, no studies have yet shown a functional association of CA I or XIII with membrane transporters, and even those associations that have been shown for CA II are hotly debated (Becker et al., 2014; Lu et al., 2006; Piermarini et al., 2007). A clue could instead come from glucose-6 phosphate dehydrogenase deficiency, which both induces hemolytic anemia and is correlated with significantly reduced CA I mRNA transcript abundance in humans (Kuo et al., 2005). This may suggest that CA I plays a peripheral role in the pentose phosphate pathway or other aspects of cellular metabolism—a role that would be presumably co-opted by CA XIII in squamate reptiles. While this is clearly speculation, the present results suggest the physiological function of erythrocyte CA XIII in pythons is not predominantly gas transport.

Acknowledgments

Financial support for this work was provided by the Natural Science Foundation (NSF) grants to M. Grosell (IOS 11466695), S. Secor (IOB-0466139) and A.J. Esbaugh (EF-1315290). MG is Maytag Professor of Ichthyology. Care of, and experimentation on snakes was approved by the Institutional Animal Care and Use Committees of both the University of Alabama and the University of Miami.

References

Becker, H.M., Klier, M., Deitmer, J.W., 2014. Carbonic anhydrases and their interplay with acid/base-coupled membrane transporters. Subcell. Biochem. 75, 105–134.
Boone, C.D., Pinard, M., McKenna, R., Silverman, D., 2014. Catalytic mechanism of alpha-class carbonic anhydrases: CO_2 hydration and proton transfer. Subcell. Biochem. 75, 31–52.
Brinkman, R., Margaria, R., Meldrum, N.U., Roughton, F.J.W., 1932. The CO_2 catalyst present in blood. J. Physiol. Lond. 75, 3–4.
Chegwidden, W.R., Carter, N.D., 2000. Introduction to the carbonic anhydrases. In: Chegwidden, W.R., Carter, N.D., Edwards, Y.H. (Eds.), The Carbonic Anhydrases: New Horizons. Birkhauser Verlag Basel, Boston, pp. 13–28.
Dixon, M., 1953. The determination of enzyme inhibitor constants. Biochem. J. 55, 170–171.
Easson, L.H., Stedman, E., 1937. The absolute activity of choline-esterase. Proc. R. Soc. Lond. B 121, 142–164.
Ellory, J.C., Wolowyk, M.W., Young, J.D., 1987. Hagfish (*Eptatretus stouti*) erythrocytes show minimal chloride transport activity. J. Exp. Biol. 129, 377–383.
Eriksson, A.E., Kylsten, P.M., Jones, T.A., Liljas, A., 1988. Crystallographic studies of inhibitor binding sites in human carbonic anhydrase II: a pentacoordinated binding of the SCN^- ion to the zinc at high pH. Proteins 4, 283–293.
Esbaugh, A.J., Tufts, B.L., 2006a. Evidence of a high activity carbonic anhydrase isozyme in the red blood cells of an ancient vertebrate, the sea lamprey (*Petromyzon marinus*). J. Exp. Biol. 209, 1169–1178.
Esbaugh, A.J., Tufts, B.L., 2006b. The structure and function of carbonic anhydrase isozymes in the respiratory system of vertebrates. Respir. Physiol. Neurobiol. 154, 185–198.
Esbaugh, A.J., Lund, S.G., Tufts, B.L., 2004. Comparative physiology and molecular analysis of carbonic anhydrase from the red blood cells of teleost fish. J. Comp. Physiol. B. 174, 429–438.
Esbaugh, A.J., Perry, S.F., Bayaa, M., Georgalis, T., Nickerson, J., Tufts, B.L., Gilmour, K.M., 2005. Cytoplasmic carbonic anhydrase isozymes in rainbow trout *Oncorhynchus mykiss*: comparative physiology and molecular evolution. J. Exp. Biol. 208, 1951–1961.
Esbaugh, A.J., Gilmour, K.M., Perry, S.F., 2009. Membrane-associated carbonic anhydrase in the respiratory system of the Pacific hagfish (*Eptatretus stouti*). Respir. Physiol. Neurobiol. 166, 107–116.
Ferreira, R., Ohneda, K., Yamamoto, M., Philipsen, S., 2005. GATA1 function, a paradigm for transcription factors in hematopoiesis. Mol. Cell. Biol. 25, 1215–1227.
Frost, S.C., 2014. Physiological functions of the alpha class of carbonic anhydrases. Subcell. Biochem. 75, 9–30.

Gilmour, K.M., Thomas, K., Esbaugh, A.J., Perry, S.F., 2009. Carbonic anhydrase expression and CO_2 excretion during early development in zebrafish *Danio rerio*. J. Exp. Biol. 212, 3837–3845.
Greene, H.W., 1997. Snakes: The Evolution of Mystery in Nature. California Press, Berkeley.
Hall, G.E., Schraer, R., 1979. Purification and partial characterization of high and low activity carbonic anhydrase isoenzymes from *Malaclemys terrapin centrata*. Comp. Biochem. Physiol. 63B, 561–567.
Henry, R.P., 1991. Techniques for measuring carbonic anhydrase activity in vitro. In: Dodgson, S.J., Tashian, R.E., Gros, G., Carter, N.D. (Eds.), The Carbonic Anhydrases: Cellular Physiology and Molecular Genetics. Plenum, New York, pp. 119–131.
Henry, R.P., 1996. Multiple roles of carbonic anhydrase in cellular transport and metabolism. Annu. Rev. Physiol. 58, 523–538.
Hewett-Emmett, D., 2000. Evolution and distribution of the carbonic anhydrase gene families. In: Chegwidden, W.R., Carter, N.D., Edwards, Y.H. (Eds.), The Carbonic Anhydrases: New Horizons. Birkhauser Verlag, Boston, pp. 29–76.
Hewett-Emmett, D., Tashian, R.E., 1996. Functional diversity, conservation, and convergence in the evolution of the alpha-, beta-, and gamma-carbonic anhydrase gene families. Mol. Phylogenet. Evol. 5, 50–77.
Hicks, J.W., Bennett, A.F., 2004. Eat and run: prioritization of oxygen delivery during elevated metabolic states. Respir. Physiol. Neurobiol. 144, 215–224.
Innocenti, A., Lehtonen, J.M., Parkkila, S., Scozzafava, A., Supuran, C.T., 2004. Carbonic anhydrase inhibitors. Inhibition of the newly isolated murine isozyme XIII with anions. Bioorg. Med. Chem. Lett. 14, 5435–5439.
Kuo, W.H., Yang, S.F., Hsieh, Y.S., Tsai, C.S., Hwang, W.L., Chu, S.C., 2005. Differential expression of carbonic anhydrase isoenzymes in various types of anemia. Clin. Chim. Acta 351, 79–86.
Lehtonen, J., Shen, B., Vihinen, M., Casini, A., Scozzafava, A., Supuran, C.T., Parkkila, A.K., Saarnio, J., Kivela, A.J., Waheed, A., Sly, W.S., Parkkila, S., 2004. Characterization of CA XIII, a novel member of the carbonic anhydrase isozyme family. J. Biol. Chem. 279, 2719–2727.
Lindskog, S., Silverman, D., 2000. The catalytic mechanism of mammalian carbonic anhydrase. In: Chegwidden, W.R., Carter, N.D., Edwards, Y.H. (Eds.), The Carbonic Anhydrases: New Horizons. Birkhauser Verlag, Basel.
Lu, J., Daly, C.M., Parker, M.D., Gill, H.S., Piermarini, P.M., Pelletier, M.F., Boron, W.F., 2006. Effect of human carbonic anhydrase II on the activity of the human electrogenic Na/HCO_3 cotransporter NBCe1-A in Xenopus oocytes. J. Biol. Chem. 281, 19241–19250.
Lund, S.G., Dyment, P., Gervais, M.R., Moyes, C.D., Tufts, B.L., 2002. Characterization of erythrocyte carbonic anhydrase in an ancient fish, the longnose gar (*Lepisosteus osseus*). J. Comp. Physiol. B. 172, 467–476.
Magid, E., 1967. The activity of carbonic anhydrase B and C from human erythrocytes and the inhibition of the enzymes by copper. Scand. J. Haematol. 4, 257–270.
Maren, T.H., Parcell, A.L., Malik, M.N., 1960. A kinetic analysis of carbonic anhydrase inhibition. J. Pharmacol. Exp. Ther. 130, 389–400.
Maren, T.H., Rayburn, C.S., Liddell, N.E., 1976. Inhibition by anions of human red cell carbonic anhydrase B: physiological and biochemical implications. Science 191, 469–472.
Meldrum, N.U., Roughton, F.J.W., 1933. Carbonic anhydrase: its preparation and properties. J. Physiol. Lond. 80, 113–142.
Mitchell, R.T., Henry, R.P., 2014. Carbonic anhydrase induction in euryhaline crustaceans is rate-limited at the post-transcriptional level. Comp. Biochem. Physiol. A Mol. Integr. Physiol. 169, 15–23.
Perry, S.F., Esbaugh, A., Braun, M., Gilmour, K.M., 2009. Gas transport and gill function in water-breathing fish. In: Glass, M.L., Wood, S.C. (Eds.), Cardio-Respiratory Control in Vertebrates. Springer-Verlag, Berlin, pp. 5–42.
Pfaffl, M.W., 2001. A new mathematical model for relative quantification in real-time RT-PCR. Nucleic Acids Res. 29, 45.
Piermarini, P.M., Kim, E.Y., Boron, W.F., 2007. Evidence against a direct interaction between intracellular carbonic anhydrase II and pure C-terminal domains of SLC4 bicarbonate transporters. J. Biol. Chem. 282, 1409–1421.
Pope, C.H., 1961. The Giant Snakes. Knopf, New York.
Sanyal, G., 1984. Comparative carbon dioxide hydration kinetics and inhibition of carbonic anhydrase isozymes in vertebrates. Ann. N. Y. Acad. Sci. 165–178.
Secor, S.M., Diamond, J., 1995. Adaptive responses to feeding in Burmese pythons: pay before pumping. J. Exp. Biol. 198, 1313–1325.
Secor, S.M., Nagy, K.A., 1994. Bioenergetics correlates of foraging mode for the snakes *Crotalus cerastes* and *Masticophis flagellum*. Ecology 1600–1614.
Secor, S.M., Hicks, J.W., Bennett, A.F., 2000. Ventilatory and cardiovascular responses of a python (*Python molurus*) to exercise and digestion. J. Exp. Biol. 203, 2447–2454.
Slip, D.J., Shine, R., 1988. Feeding habits of the diamond python, Morelia s. spilota: ambush predation by a boid snake. J. Herpetol. 323–330.
Stabenau, E.K., Heming, T., 2003. Pulmonary carbonic anhydrase in vertebrate gas exchange organs. Comp. Biochem. Physiol. A Mol. Integr. Physiol. 136, 271–279.
Stabenau, E.K., Vietti, K.R., 2002. Pulmonary carbonic anhydrase in the garter snake, *Thamnophis sirtalis*. Physiol. Biochem. Zool. 75, 83–89.
Stabenau, E.K., Bidani, A., Heming, T.A., 1996. Physiological characterization of pulmonary carbonic anhydrase in the turtle. Respir. Physiol. 104, 187–196.
Swenson, E.R., 2000. Respiratory and renal roles of carbonic anhydrase in gas exchange and acid base regulation. In: Chegwidden, W.R., Carter, N.D., Edwards, Y.H. (Eds.), The Carboic Anhydrases: New Horizons. Birkhauser Verlag, Boston, pp. 281–342.
Tufts, B., Perry, S.F., 1998. Carbon dioxide transport and excretion, Fish Physiology. Fish Respiration vol. 17. Academic Press, San Diego, pp. 229–282.
Tufts, B.L., Bagatto, B., Cameron, B., 1992. *In vivo* analysis of gas transport in arterial and venous blood of the sea lamprey, *Petromyzon marinus*. J. Exp. Biol. 169, 105–119.
Yang, H., Hewett-Emmett, D., Tashian, R.E., 2000. Absence or reduction of carbonic anhydrase II in the red cells of the beluga whale and llama: implications for adaptation to hypoxia. Biochem. Genet. 38, 241–252.